Self-Aggregation of Amphiphilic Cationic Polyelectrolytes Based on Polysaccharides

Marieta Nichifor,*,†,‡ Sonia Lopes,† Margarida Bastos,§ and Antonio Lopes†

Instituto de Tecnologia Quimica e Biologica (ITQB/UNL), P-2781-901 Oeiras, Portugal, "Petru Poni" Institute of Macromolecular Chemistry, 700487 Iasi, Romania, and CIQ (UP), Department of Chemistry, Faculty of Sciences, University of Porto, P-4169-007 Porto, Portugal

Received: June 23, 2004

The self-aggregation of polyelectrolytes having *N*-alkyl-*N*,*N*-dimethyl-*N*-(2-hydroxypropyl)ammonium chloride pendant groups (alkyl = octyl, dodecyl, or cetyl) randomly distributed along a polysaccharide backbone (dextran) was studied by steady-state fluorescence techniques using several free fluorescent probes or pyrene-labeled polymers and by viscometry. The onset, offset, and highest values of the fluorescence response of *N*-phenylnaphthylamine (NPN), pyrene (Py), and 1,6-diphenyl-3,5,6-hexatriene (DPH) were corroborated with NPN and DPH anisotropy and quenching experiments to describe the dynamic of hydrophobic microdomain formation and microdomain characteristics. The start of the aggregation process (critical aggregation concentration, cac) and the microdomain characteristics such as polarity, microviscosity, size, and number strongly depend on the alkyl chain length and the degree of substitution with cationic pendant groups. Fluorescence experiments with pyrene-labeled polymers and viscosity data suggest that microdomains are mainly formed by intramolecular hydrophobic associations, except for the polymers carrying octyl groups, where some intermolecular associations were revealed.

Introduction

Amphiphilic polymers are very interesting materials for scientists because of their resemblance to biological macromolecules and their potential applications as water-born paints and coatings, cosmetics, food and personal care goods, and drug delivery systems and in oil recovery and water treatments.[1−5] Among different types of polymeric amphiphiles, hydrophobically modified water-soluble polymers with hydrophobes located on side chains have received special attention. These polymers can form aggregates because of hydrophobic interactions within the same polymer chain (intramolecular association) or between different chains (intermolecular association). The final micro- and macrostructure of the aggregates depends on the chemical structure and the physicochemical properties of the polymers. In the case of hydrophobically modified polyelectrolytes where the hydrophobic interactions are in competition with the electrostatic repulsion between charged sites, the final polymer architecture is governed by the charge density, the relative ratio, and the position of the charges and hydrophobes with respect to the polymer's main chain.[5−9] Amphiphilic polyelectrolytes that are obtained by chemical modification of water-soluble polymers can have the hydrophobes distributed either randomly or as blocks along the polymer backbone. The charges and hydrophobes can be located in different positions or can belong to the same side chain. In the latter case, we have low molecular amphiphiles bound as side groups to a polymeric backbone via either their headgroup or hydrophobic tail. All of these characteristics can significantly influence the final conformational characteristics and aggregate architecture of amphiphilic polyelectrolytes.[5−7,9−12]

During past decades, many studies have been devoted to the synthesis and characterization of hydrophobically modified polyelectrolytes. Charged polymers carrying mainly long-chain hydrocarbons, but also fluorocarbons,[12,13] and cyclic compounds[14−16] as well as polysiloxanes[17] and even twin hydrocarbons[18] as hydrophobes were prepared and characterized by a variety of methods including light scattering,[15,19−21] fluorescence techniques,[8,9,11,21−29] surface tension,[13,27,30] microcalorimetry,[31−33] ultrasound techniques,[34] viscometry,[13,18,20,29,35] NMR,[17,25,36] and electron-spin resonance spectroscopy.[26,35] Theoretical models for the association of such polymers were also published.[37,38] Among the characterization methods, fluorescence techniques represent a powerful procedure, enabling the researcher to determine many aggregate characteristics by using appropriate free fluorescent probes or probe-labeled polymers.[39,40]

The aim of the present study is to analyze in detail the aggregate building process and the characteristics of the aggregates formed in salt-free aqueous solutions of new hydrophobically modified cationic polymers based on polysaccharides carrying pendant *N*-alkyl-*N*,*N*-dimethyl-*N*-(2-hydroxypropyl)ammonium chloride groups, where alkyl is an octyl, dodecyl, or cetyl group (Scheme 1) and the polysaccharide is dextran. These pendant groups can be considered to be head-attached cationic surfactants that are randomly distributed along the polysaccharide backbone. Various fluorescence techniques and several fluorescent probes were used to characterize the self-aggregates (hydrophobic microdomains) that were formed by these polymers as a function of their chemical composition and concentration. To obtain supplementary information about the aggregation, we also studied the same polymers that were labeled with pyrene and their fluorescence. Some viscometric measurements were performed as well. All experiments were

* Corresponding author. Address: "Petru Poni" Institute of Macromolecular Chemistry, Aleea Grigore Ghica Voda 41 A, 700487 Iasi, Romania. Tel: +40-232-260333. Fax: +40-232-211299. E-mail: nichifor@icmpp.ro.

† Instituto de Tecnologia Quimica e Biologica.

‡ "Petru Poni" Institute of Macromolecular Chemistry.

§ University of Porto.

10.1021/jp047267v CCC: $27.50
Published on Web 09/28/2004

SCHEME 1: Chemical Structure of Cationic Amphiphilic Polyelectrolytes Obtained by Chemical Modification of Dextran. R = Octyl (C_8), Dodecyl (C_{12}) or Cetyl (C_{16}). DS = $100x/(x + y)$

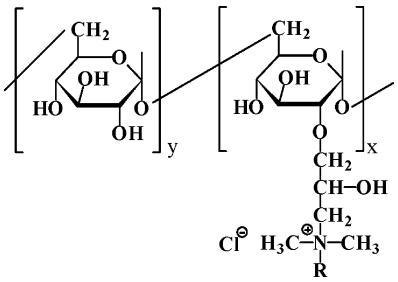

carried out in dilute and semidilute solutions at concentrations up to 1−2 g/dL, below the critical overlapping concentration of native dextran (about 5 g/dL).

Experimental Section

Materials. The dextran sample (D40) was supplied by Sicomed S. A. Bucharest and had $M_w = 40\,000$ and $M_w/M_n = 1.12$, as determined by capillary viscometry and static light scattering. *N*-phenylnaphthylamine (NPN), pyrene (Py), and 1,6-diphenyl-3,5,6-hexatriene (DPH) were from Sigma and were used after appropriate recrystallization. Cetylpyridinium bromide (CPB), 1-pyrenebutyric acid (Py-BuCOOH), *N*,*N*-dimethylaminopyridine (DMPA), and *N*,*N*-dicyclohexylcarbodiimide (DCC) were obtained from Aldrich and were used as received. Doubly distilled deionized water obtained with an Elgastat UHQ PS purification system was used for the preparation of aqueous solutions.

Cationic Polymers with Pendant Quaternary Ammonium Groups Synthesis. These cationic polymers were synthesized by chemical modification of dextran. The synthesis of a polymer having dimethyloctylammonium chloride side groups is presented here as a typical example. Dextran D40 was dissolved in deionized water, and a mixture of epichlorohydrin and *N*,*N*-dimethyl-*N*-octylamine (both from Aldrich) was added and then the resulting solution was stirred for 6 h at 70 °C. The polymer was recovered from the reaction mixture by precipitation in acetone and then purified by repeated precipitation and finally by sequential dialysis against 0.1 N HCl and water. Dialysis tubing with a cutoff of 12 000 from Sigma was used for this purpose. Liofilization of the diluted water solution that was obtained after dialysis provided the final polymer as a white powder. The chemical structure was proven by ^{1}H NMR and elemental analysis. The content in amino groups (degree of substitution, DS) was determined from the nitrogen (elemental analysis) and chloride-ion content (potentiometric titration with $AgNO_3$) and was found to be 28.1 mol % (moles amino groups per 100 glucopyranosidic units). DS = $100x/(x + y)$, where x and y are the molar fraction of substituted and unsubstituted glucosidic units, respectively.

The polymer belongs to a series of cationic polysaccharides with a general code PzM−RX, where Pz means the polysaccharide (D for dextran), M is the molecular weight of the polysaccharide, and R is the substituent at amino group, according to Scheme 1 (R = Oct (C_8), Dod (C_{12}), and Cet (C_{16})) and X = DS ± 2−3 mol %. Accordingly, the code for the sample synthesized as described above is D40−Oct30.

Cationic Polymers Containing a Pyrene Moiety as a Fluorescent Label. These cationic polymers were prepared as follows. D40 (1 g), Py-BuCOOH (0.08 g), and DMAP (0.004 g) were dissolved in a mixture of *N*-methylformamide/DMF 1/0.9 v/v and then DCC (0.0286 g) dissolved in DCM was added, and the mixture was stirred at room temperature for 24 h. The reaction mixture was filtered, and the polymer was purified by repeated precipitation from *N*-methylformamide in methanol and was dried under vacuum. The content of pyrene bound to the polymer was estimated from the absorbance at 344 nm and the extinction coefficient of Py−BuCOOH ϵ (344 nm) = 37 600 M^{-1} cm^{-1}. All absorbance measurements were performed in 0.1 M SDS solutions to avoid pyrene−pyrene associations.[41] The labeled dextran was aminated under the conditions described in the previous paragraph, and the purification was performed by sustained dialysis until no pyrene derivative was found in the dialysis solution. The two polymers prepared under these conditions, D40−Oct30−Py and D40−Dod30−Py, had a Py content of about 9×10^{-6} mol/g polymer, corresponding to an average of 0.35 mol pyrene/polymer chain.

Methods. *Preparation of Polymer Stock Solutions for Fluorescence Measurements.* The polymer stock solutions were prepared in a 1×10^{-6} M aqueous solution of NPN or Py and were diluted to the desired concentration with the corresponding fluorophore solution. When DPH was used, a stock solution of 1×10^{-3} M fluorophore in methanol was prepared, and aliquots of this solution were added to empty vials in such an amount to obtain a final DPH concentration of 1×10^{-6} M. The methanol was evaporated, and polymer solutions of known concentrations were added to vials. All of the mixtures were left under mild shaking for 24 h to equilibrate.

Quenching Experiments. We performed quenching experiments with Py as a fluorescent probe (1×10^{-6} M) and CPB as a quencher (0.01−0.1 mM). A stock solution of CPB (1 mM in methanol) was prepared, and aliquots of this solution were added to empty vials in the amount required for the final CPB concentration. Methanol was evaporated and then a polymer solution with a known concentration, prepared in 1×10^{-6} M Py, was added to each vial. The mixtures were left to equilibrate under mild shaking for 24 h.

Instruments. Steady-state fluorescence spectra and fluorescence anisotropy values were obtained with a SPEX Fluorolog 212 in L conformation with slits set to 1 mm. In the case of emission spectra, the excitation wavelengths were 340 nm (NPN), 337 (Py), and 360 (DPH). Excitation spectra of pyrene were obtained with emission wavelength fixed at 390 nm. In the case of fluorescence anisotropy, the emission wavelength was set at 430 nm for both NPN and DPH; the instrumental correction factor, $G = I_{HV}/I_{HH}$ was determined by the method of Azumi and McGlynn.[42] All fluorescence measurements were performed at ambient temperature.

Capillary viscometry was performed with Ubbelhode viscometers with different capillary constants that were immersed in a thermostated bath at 25.0 ± 0.1 °C. Kinematic viscosities (in cst) were calculated as $\eta = t \times k$, where t is the flow time of polymer solution in seconds and k is the capillary constant in mm^2 s^2.

Results and Discussion

Different fluorescent probes can provide different information about the hydrophobic domain characteristics, such as micropolarity and microviscosity.[39,40] To obtain as much information as possible, we used three fluorescent probes, NPN, Py, and DPH, for the characterization of the hydrophobic domains of the polymers.

NPN is a fluorescent probe with moderate hydrophobicity, which was frequently used in biology for measurements of membrane permeability induced by different biological events[43−45]

and also in the characterization of the aggregates formed by surfactants[46] or amphiphilic polymers.[47] Its known ability to change the emission intensity maximum and to undergo a batochromic shift of this maximum with decreasing polarity and increasing viscosity of the environment was used for the characterization of amphiphile aggregates. Unlike its more frequently used sulfonate derivative (ANS) that is bound preferentially to the hydrophilic surface of the micelles NPN partitions deeper into the hydrophobic part of the micelles.[44]

Py is the most used fluorescent probe because of its long fluorescence lifetime, the sensitivity of its fine structure of emission and excitation spectra to microenvironment polarity, and its efficient excimer formation.[40,48] In the case of the emission spectra, the relative intensities of the first and third vibronic peaks (I_1/I_3 or I_3/I_1) are sensitive to environment polarity and are frequently used for the determination of aggregate polarity; the variation of these properties with amphiphile concentration were used for cac calculation. The variation of the intensity of the first vibronic peak (I_1) of emission spectra has also been used.[49,50] Several authors[9,49,50] have used the excitation spectra of Py, which are considered more sensitive to aggregate formation, because the emission spectra could be influenced by the excitation wavelength. In excitation spectra, a shift of the (0, 0) band from 333 to 338 nm with decreasing polarity of the environment was noticed. Consequently, the ratio I_{338}/I_{333} can be used to characterize the polarity of a microdomain. Pyrene is also used for the determination of the aggregation number of micelles due to the ability of many compounds to quench its emission intensity. Finally, there are many studies where Py is covalently bound to a polymer as a label to obtain more information about the self-aggregation of amphiphilic polymers.[8,15,28,29,51−53]

DPH is a very hydrophobic probe that has almost no fluorescence in aqueous solution (it is practically water insoluble), but it is highly fluorescent in a hydrophobic environment.[54] It was widely used for the determination of membrane microviscosity due to the sensitivity of its fluorescence polarization to rotational motion[44,45] but rarely for the determination of the cac of amphiphilic polymers.[34] Because of its insolubility and lack of fluorescence emission in water solutions, any measurable value for DPH intensity in the presence of an amphiphile will indicate the probe solubilizing into the hydrophobic microdomain of that amphiphile.

Critical Aggregation Concentration of the Polymers. Steady-state fluorescence is commonly used to determine the start of surfactant aggregation, cmc. The technique involves the use of a fluorescent probe, which partitions favorably in the hydrophobic core of the micelles. The aggregation of hydrophobic moieties of polymeric amphiphiles is considered to be micellelike, but the aggregation process and the aggregates' characteristics are different from those of low molecular-weight surfactant micelles. Hydrohobically modified polyelectrolytes with a higher content in hydrophobic moieties (>10 mol %), called polysoaps, are supposed to have a zero cmc because the hydrophobic microdomains are present at any concentration, and their content increases linearly with polymer concentration.[6,24,55] However, in some cases, the existence of a concentration below which no significant microdomain presence could be detected, was demonstrated by different methods such as fluorescence, conductivity, NMR,[9,25] and ESR.[35] The presence and the value of this critical aggregation concentration (cac) depend mostly on the chemical structure of the amphiphilic polyelectrolyte, and the specific variation of a polyelectrolyte conformation with concentration should be taken into account.[56] Therefore, we performed several fluorescence measurements to detect the presence of such a critical concentration.

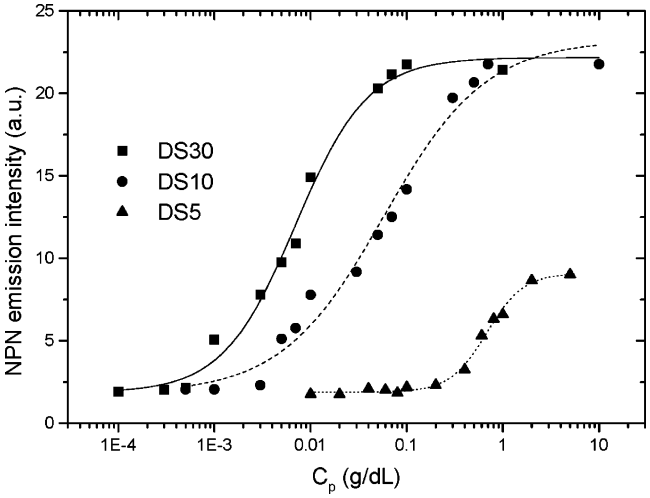

Figure 1. Variation of NPN emission intensity with concentration of cationic polymers D40−DodX, with different X (degree of substitution, DS, in mol %) values. The lines are the best sigmoidal fits to the experimental data.

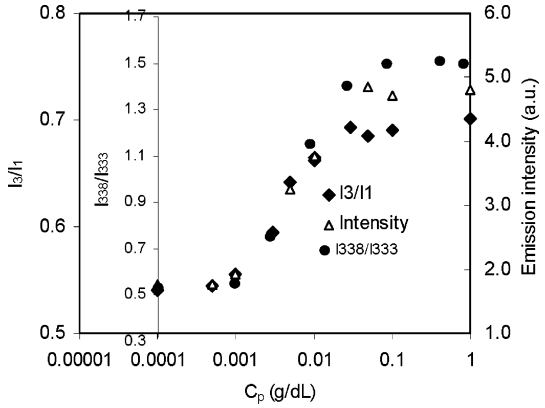

Figure 2. Fluorescence intensity I_1, intensity ratio I_3/I_1 (both from pyrene emission spectra), and I_{338}/I_{332} (from pyrene excitation spectra) as a function of the polymer D40−Dod30 concentration.

The NPN emission intensity of aqueous solutions that contain cationic amphiphilic polymers presents a significant increase at a certain polymer concentration. This increase is sigmoidal and, similar to other amphiphilic polymers,[24,36,49,57] it stretches over a large range of concentration (about 2 orders of magnitude), indicating that the aggregation process is less cooperative than in case of low-molecular-weight surfactants. An example of such a variation is presented in Figure 1 for the polymer D40−DodX. As one can see, the onset of emission intensity variation and the maximum values that we obtained for this intensity depend on the *X* value.

Figure 2 shows the variation of the Py fluorescence in response to the polymer D40−Dod30 concentration, as obtained from both emission (I_1 and I_3/I_1) and excitation spectra (I_{338}/I_{333}). Except for the upper part of the curves (C_p > 0.2 g/dL), the onset of the fluorescence property change, the slope of the change, and the offset of the change are quite similar for all types of measurements; consequently, we used for our purposes the data obtained from the emission spectra, namely, the ratio I_3/I_1. It has to be mentioned that no excimer formation was observed in emission spectra of free pyrene in the presence of all polymers under the study.

Figure 3 shows the comparative data that was obtained from the emission spectra of NPN, Py, and DPH for the cationic

TABLE 1: Critical Aggregation Concentrations (cac, in g/dL) and Partition Coefficients (K_p) Obtained from Steady-State Fluorescence Measurements[a]

	NPN			Py			DPH		
polymer	cac_1	cac_2	K_p	cac_1	cac_2	K_p	cac_1	cac_2	cac_3
D40−Oct30	0.30		1.0×10^2 (e) 4.0×10^3 (r)	0.22	3.0	6.5×10^2 (e)	0.3	3.0	
D40−Dod30	0.0009	0.0643	5.5×10^4 (e) 9.5×10^4 (r)	0.0009	0.01	1.0×10^5 (e)	0.0008	0.01	0.1
D40−Cet30	0.00023	0.030	9.0×10^4 (e) 1.5×10^5 (r)	0.0003	0.009	1.5×10^5 (e)	0.0002	0.01	0.1
D40−Cet15	0.001	0.070	5.0×10^4 (e)	0.001	0.02	9.5×10^4 (e)	0.0008	0.01	0.1

[a] Partition coefficients of the fluorescent probes were obtained either from emission data (e) or ansiotropy data (r).

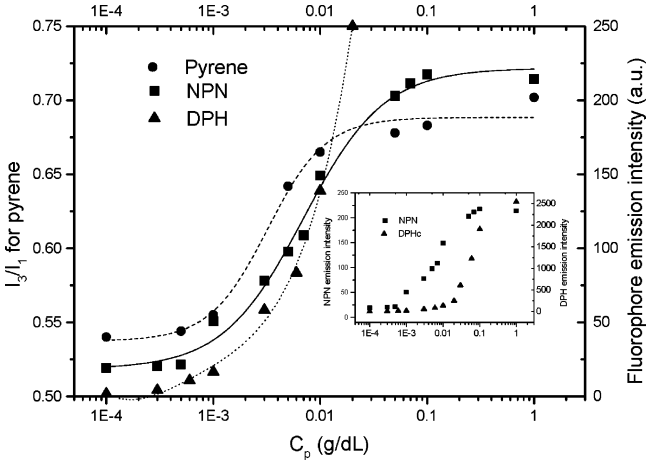

Figure 3. Variation of fluorescence properties of fluorophores with concentration of the cationic polymer D40−Dod30. The lines are the sigmoidal fits to the experimental data. (Inset) DPH emission intensity variation over the entire polymer concentration range.

polymer D40−Dod30. The onset of the probe's property change is set in all cases at about 0.001 g/dL. The changes stretch over a large concentration range, and the end of the change (the offset of the fluorescence property change) differs for the three fluorophores, especially for very hydrophobic DPH. The difference in the values for the offset polymer concentration that was noticed for NPN and Py is small, but in case of DPH, a much sharper increase in its emission intensity occurs almost when the variation of the other probe properties are already leveled (inset in Figure 3). This different behavior can be explained by intrinsic probe hydrophobicity. NPN and Py are hydrophobes with some water solubility. The variation in their fluorescence properties is due to a sequential partition of the probe between water (where they are solubilized) and hydrophobic microdomains that is present until equilibrium between the two regions (or probe saturation) occurs. The variation of DPH emission intensity is only due to the progressive solubilization of the probe in microdomains. Perhaps the size of the genuine domains is low and their polarity is still too high; thus, they can solubilize only low amounts of DPH. However, when the process of aggregation reaches a certain level, the domains become large and hydrophobic enough that can solubilize a much larger amount of the probe, resulting in a sharper increase in DPH emission intensity. A leveling of the solubilization process is attained only at a much higher polymer concentration than in the case of the other more hydrophilic probes.

There are doubts about the correct determination of the cac values from the fluorescence data due to the large concentration range over which the fluorophore response stretches. The onset and offset of the fluorophore significant response to polymer concentration variation or the midpoint of this variation were proposed to be cac.[22,25,49,57] In the present study, the similar polymer concentration corresponding to the initial response of all fluorophores used, irrespective of their chemical structure and hydrophobicity, and the sensitivity of this initial response to the chemical structure of the polymers, indicate that a significant event takes place at that particular concentration. This event can be an incipient association of side-chain hydrophobes (perhaps the very first association of two hydrophobes). As a consequence, the onset of the fluorophore response to the polymer concentration is considered here to be the first critical aggregation concentration (cac_1), having the meaning of the very beginning of the hydrophobe association (by intra- or intermolecular association). It is worth mentioning here that in the case of the D40-Oct30 a cac value of 0.5 g/dL, very close to that determined by fluorescence measurements (0.3 g/dL), was found by microcalorimetry.[33] Above cac_1, the association process (microdomain formation) continues over a large range of polymer concentration and then a leveling of the fluorescence response is established; this time, the leveling concentration depends on the nature of the fluorophore, which means on its partition or solubilization into microdomains. The offset of the transition process, which depends on the fluorophore chemical nature, could be assigned to the equilibrium reached by the system or to a saturation of aggregates with fluorophore. This concentration was denoted as cac_2, which does not correspond until practically to the end of the aggregation process (as we will show in this paper). The concentration values at the beginning and the end of the fluorophore property change are listed in Table 1 for some of the tested polymers. In case of DPH, cac_2 corresponds to the start of the sharper increase in the DPH fluorescence emission and the offset of the probe response was noted as cac_3.

The values of the fluorophore response that were determined in aqueous solution containing 1 g/dL of polymer are listed in Table 2. At that concentration, all polymers under study are in the range where the fluorescence responses become constant (limiting values). From these data, it is obvious that the microdomain polarity (Py intensity ratio and NPN intensity), microviscosity (NPN intensity), and solubilization ability (DPH intensity) depend on the length of the R substituent and the degree of substitution. The increase in the length of the R substituent results in a lower polarity and a higher solubilization ability of microdomains, the most evident jump in these properties being noticed between C_8 and C_{12}. The polarity given by pyrene, I_3/I_1 (0.7−0.76), is comparable with those obtained for other amphiphilic cationic polymers[55] but is higher than that found for a low-molecular-weight surfactant like SDS or for poly(acrylic acid) modified with *n*-octylacrylate.[26]

The influence of the degree of substitution and the length of the R substituent on cac_1 (calculated in the presence of NPN)

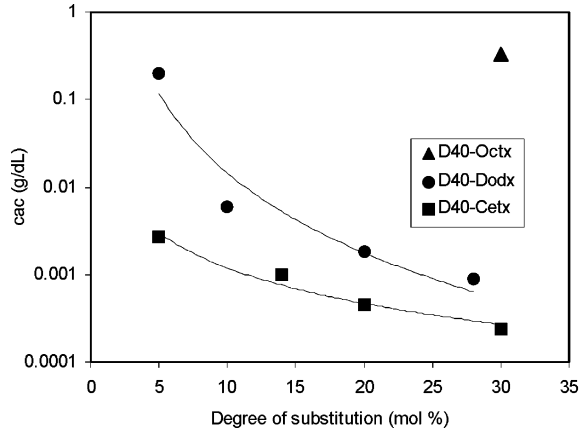

Figure 4. Variation of critical aggregation concentration (cac_1) with the degree of substitution of the cationic polymers as a function of the length of R in the polymer D40−RX. The lines are only guides for the eye.

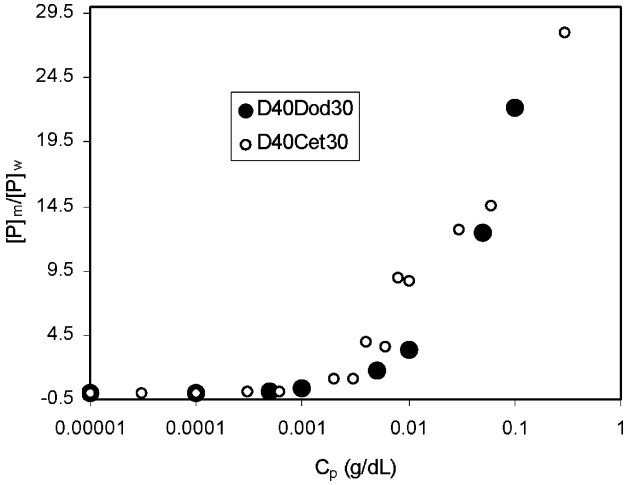

Figure 5. Variation of the ratio $[P]_m/[P]_w$ with polymer concentration, as estimated from the pyrene emission data (I_3/I_1).

is shown in Figure 4. The values of cac_1 decrease sharply with increasing R length and DS.

Fluorophore Partition Coefficients. In the case of polymeric amphiphiles with pendant amphiphilic groups (or polysoaps), the sigmoidal change in the fluorescent probe's property with concentration might be assigned to a partition of the probe between water and hydrophobic microdomains that were formed by the association of pendant groups.[24,49,50]

We have used the data resulting from the emission experiments performed in the presence of NPN or Py for the study of the fluorophore partition. It was assumed that the fluorophore response (F), that is, the NPN emission intensity or the Py intensity ratio I_3/I_1, depends on the ratio between the concentration of the probe in water, $[P]_w$, and in microdomains, $[P]_m$. The lowest probe fluorescence response, F_{min}, corresponds to the complete partition of the probe in water, and the highest probe fluorescence property, F_{max}, corresponds to the probe completely dissolved in hydrophobic microdomains. In this case, the ratio of the probe in microdomain and water is given by eq 1[24,49]

$$\frac{[P]_m}{[P]_w} = \frac{F - F_{min}}{F_{max} - F} \tag{1}$$

Under the presumption of simple partition equilibrium of the probe between water and microdomains, the ratio of the probe concentrations in the two regions can be related to the equilibrium partition constant (K_p) using eq 2

$$\frac{[P]_m}{[P]_w} = K_p x_m \tag{2}$$

where K_p is the partition coefficient and x_m is the volume fraction of hydrophobes. If we assume a proportional increase in hydrophobic microdomains with polymer concentration (C_p, g/dL), then x_m can be calculated with eq 3

$$x_m = \frac{C_p f_H}{100 d_H} \tag{3}$$

where f_H is the fraction of hydrophobe in the polymer and d_H is the density of the hydrophobic microdomains (g/mL).

Consequently, the variation of the fluorescence property of a probe with polymer concentration can be expressed as

$$F = \frac{F_{min} + x_m K_p F_{max}}{1 + K_p x_m} \tag{4}$$

With the assumption of a linear increase in hydrophobic microdomain with concentration, the plot of the ratio $[P]_m/[P]_w$ as a function of C_p should give a straight line with a slope of K_p. However, as Figure 5 shows, there are breaks in the plots, and the initial linear part (where the amount of Py in microdomains is close to zero) stretches over 2 orders of magnitude. The start of the increase in the ratio $[P]_m/[P]_w$ occurs at a concentration close to cac_1. These data support the assumption that below cac_1 no measurable hydrophobe association takes place.[17,19,25]

The calculation of K_p from the slope of the increasing part of the plots such as those in Figure 5 is not accurate because this increase is not strictly linear. Therefore, we tried to fit eq 4 to the experimental data obtained with NPN and Py by using K_p as an adjustable parameter. The values of x_m were calculated by taking d_H to be the density of the octane, dodecane, or hexadecane, according to the length of the R substituent in the polymer. The best fits for polymers D40−R30 are presented in Figure 6a and b (solid lines). The fittings are moderate, and the worst fits were obtained for D40−Oct30, both for NPN and Py. We have supposed that this is due to the fact that x_m is not

TABLE 2: Properties of Aqueous Solutions of Cationic Polymers at Polymer Concentration 1 g/dL

polymer	viscosity cst	anisotropy, *r* NPN	anisotropy, *r* DPH	I_3/I_1 (pyrene)	$10^{-5}\times$ NPN emission intensity	$10^{-6}\times$ DPH emission intensity	*M*/chain	N_{agg}
D40−Oct30	1.70	0.080	0.140	0.606	0.505	0.156	1	71
D40−Dod30	1.02	0.088	0.183	0.702	2.210	2.743	3.4	20
D40−Cet30	1.00	0.096	0.225	0.762	2.692	3.350	2.5	30
D40−Dod10	1.04				2.180		0.7	25
D40−Dod5	1.10				0.658		0.5	26
D40−Cet15	0.98	0.086	0.211	0.705	2.150	2.286	1.5	25
D40−Cet5	1.08				2.150		0.5	26

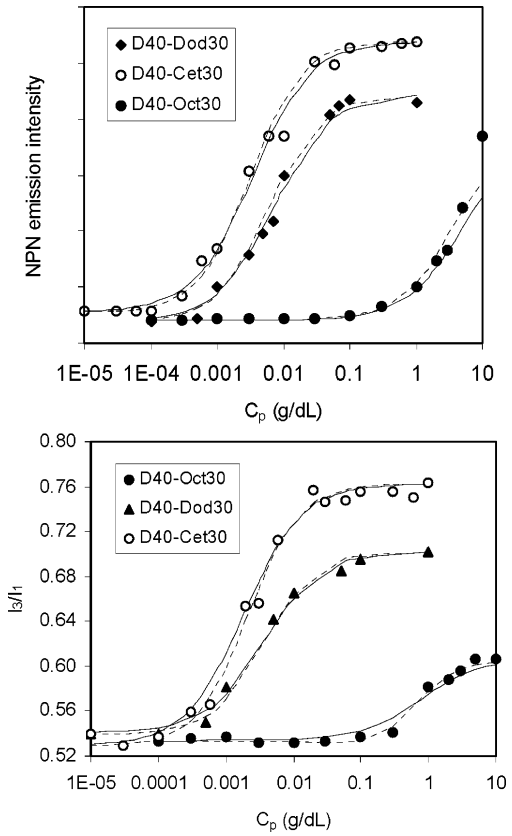

Figure 6. Variation of the NPN and Py fluorescence properties with polymer concentration. The lines are the best fits of eq 4 to the experimental data, obtained with x_m calculated according eq 3 (—), and $x_{m,corr}$ calculated with eq 5 (- - -). Dotted lines were obtained with the values of K_p that are included in Table 1.

strictly proportional to C_p. This supposition stems from the experimental data reported for the increase in hydrophobes implied in microdomains with increase in concentration of a hydrophobically modified poly(acrylic acid).[25] Our own calculation of those reported data indicated a relationship of the type described by eq 5. We tried to fit eq 4 to experimental data, replacing x_m with $x_{m,corr}$ and using K_p, A, and B as variable parameters. The fits obtained (dotted lines in Figure 6a and b) are better than the previous ones, especially for lower C_p. The K_p values for both probes that correspond to those fits (Table 1) increase with increasing R chain length. The K_p values for NPN are somewhat lower than those for Py, probably because of the higher hydrohobicity of Py in comparison with NPN. It is worth mentioning that the K_p value that was calculated for the Py in the presence of the polymer with R = C_{12} (D40-Dod30) (1×10^5) is close to that previously reported for SDS (1.2×10^5).[49]

$$x_{m,corr} = x_m(A \ln C_p + B) \tag{5}$$

Fluorescence Depolarization. The degree of fluorescence depolarization of the light emitted by a probe can be related to the extent of the motion of that probe during its lifetime in the excited state. Therefore, the steady-state fluorescence polarization can be used to determine the apparent microviscosity of the probe environment.

Variation of NPN anisotropy with the polymer concentration is sigmoidal, similar to that found for NPN emission intensity, but the anisotropy values start to increase at lower polymer concentrations than was determined for NPN emission intensity. This again indicates a stepwise partition of the probe between

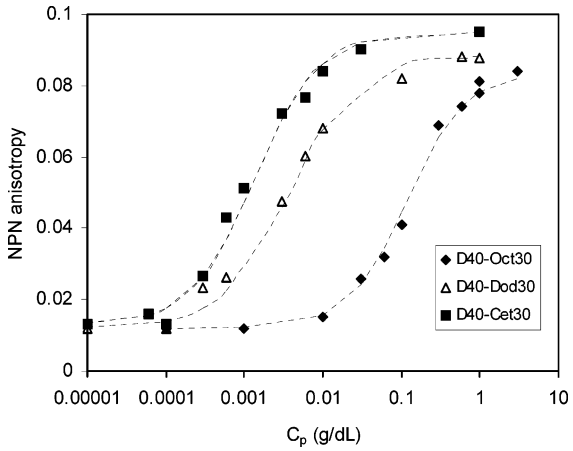

Figure 7. Steady-state fluorescence anisotropy of NPN as a function of cationic polymer concentration. The lines are the best fits of eq 6 to the experimental data, obtained for K_p values included in Table 1.

water and hydrophobic microdomains, and the partition of the probe in the system can be described by eq 6[47,58]

$$r = \frac{r_w + \dfrac{x_{m,corr}K_p r_m}{1 - x_{m,corr}}}{1 + \dfrac{x_{m,corr}K_p}{1 - x_{m,corr}}} \tag{6}$$

where K_p and $x_{m,corr}$ have the same meaning as in eqs 2 and 5 and r_w and r_m are the NPN anisotropy in water and microdomains, respectively. We tried to fit eq 6 to the experimental data (Figure 7), and the values obtained for K_p are also included in Table 1. The K_p values that were determined from anisotropy variation with polymer concentration are higher than those determined from NPN emission intensity and approach the K_p values determined for Py. This finding, together with a more sensitive variation of anisotropy with polymer concentration might be due to the different ways the two NPN properties are expressed. Thus, we can assume that the first binding of NPN takes place at the surface of the aggregates or even by attachment to a single side alkyl chain. This very early binding results in a reduction of NPN mobility (anisotropy increases), but the probe does not yet sense any change in environment polarity (no variation of emission intensity). Only after the probe is buried inside the hydrophobic microdomains does the emission intensity start to increase.

The sigmoidal increase of NPN anisotropy with an increase in polymer concentration was found for all polymer samples under study. The maximum values for anisotropy differ as a function of the R alkyl length and the degree of substitution. NPN anisotropy values for several polymers in their aqueous solutions of 1 g/dL concentration are included in Table 2. For polymers with the same DS, the anisotropy increases with increase in the R chain length, the highest anisotropy value being found for the polymer with R═C_{16}. The content in cationic amphiphilic groups determines also a variation of anisotropy.

DPH anisotropy, as determined from steady-state measurements, does not change with polymer concentration (Figure 8) even when this concentration is as low as the cac of the polymer. Because of its water insolubility, DPH anisotropy is given only by the probe molecules already solubilized inside the microdomains. Constant values of r_{DPH} were reported for other amphiphilic polymers, but the concentration range was usually that corresponding to the upper plateau in any fluorophore property variation. In our case, the constant value of r_{DPH}

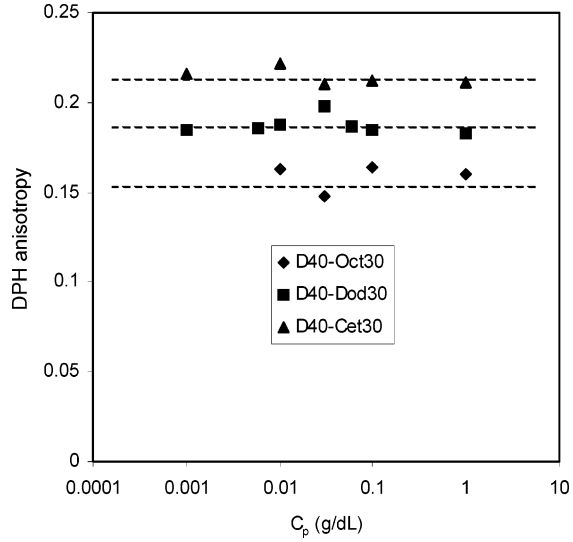

Figure 8. DPH steady-state fluorescence anisotropy as a function of cationic polymer concentration. The lines are only guides for the eye.

suggests a constant microviscosity of the hydrophobic microdomains over all of the concentrations under study, even at the incipient state of their occurrence. This could signify an increase in aggregate size and/or number with concentration, but a relatively constant compactness (microviscosity) of these aggregates where DPH resides.

Even if it is constant over a large polymer concentration range, r_{DPH} depends on the R chain length and DS, its value increasing with increasing hydrophobicity of the R substituent and DS (Table 2).

The compactness of the hydrophobic domains that are formed by the alkyl chains of amphiphilic cationic groups bound to polysaccharides is lower than that of other amphiphilic polymers. For instance, the r_{NPN} values are lower than those obtained for polymers based on dextran hydrophobically modified with bile acids (r is about 0.12−0.13) and much lower than the $r = 0.17$ determined for NPN in rigid media.[47] The values for r_{DPH} are lower than those for other cationic polymers[7] but close to the values determined for a series of maleic anhydride−coalkylvinyl ethers.[59]

Aggregation Number of Hydrophobes in Microdomains. Intramolecular aggregation of hydrophobes in amphiphilic polymers can give rise to several hydrophobic microdomains along the polymer chains,[23] according to the necklace model,[37,38] or can form a single microdomain (unimer).[14,28] Intermolecular aggregation can also occur through microdomain association connected by hydrophobic chains or unimer association (strings or globules).[19,60]

Fluorescence quenching is among the most reliable methods for the measurement of the micelle aggregation number. The method is based on the quenching of the emission of a probe by a specific quencher (Q). Both probe and quencher should have a high affinity for the micelles, and in the data analysis, one assumes a Poisson distribution of the probe and Q among the micelles. This method was used for the determination of aggregation number of hydrophobic microdomain (N_{agg}) built by amphiphilic polymers in water solution. A comparison of the N_{agg} with the number of hydrophobes per polymer chain (H_p) can give a first approximation (but not necessary a correct one) about the type of aggregation. Thus, an N_{agg} small and lower than H_p might indicate an intramolecular aggregation (necklace model).[23] When $N_{agg} \approx H_p$, a unimer seems to be the most probable aggregation form,[14,28] and an $N_{agg} > H_p$ could be proof for the occurrence of intermolecular association.[19]

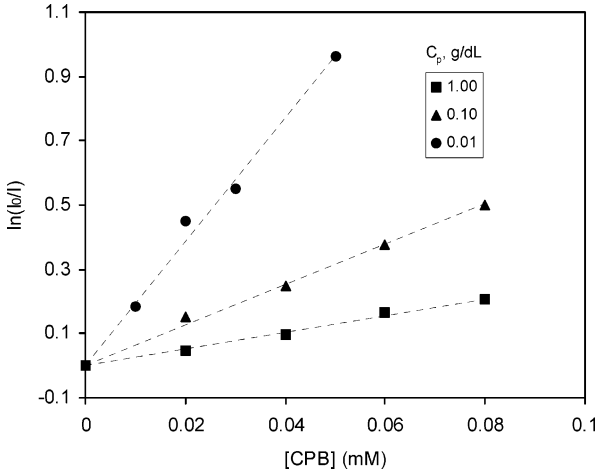

Figure 9. Variation of $\ln(I_0/I)$ as a function of CPB concentration for different concentration (C_p, g/dL) of the cationic polymer D40−Cet30.

We used CPB as the quencher for Py. It was recently demonstrated that alkylpyridinium bromides can be successfully used for the determination of the aggregation number of cationic surfactants, such as alkyltrimethylammonium halides, with the assumption that similar structures of surfactant and quencher will produce less impairment of the micelle organization by the quencher.[61] We used a low concentration of CPB (0.01−0.1 mM) to minimize a possible aggregation of this pyridinium surfactant in the presence of the cationic polymers (cmc of CPB is about 0.6 mM[62]). It has been shown that a surfactant can interact with similarly charged amphiphilic polyelectrolytes by inclusion, but its aggregation in the presence of such a polymer takes place at a surfactant concentration close to its cmc.[63,64] For the quenching experiments, we used polymer concentrations in the range where saturation with Py takes place, that is, where a constant value for I_3/I_1 was observed. Under these conditions, the Stern−Volmer plots were linear, meaning that the quenching process takes place by a single mechanism. Therefore, we have used eq 7 to calculate the microdomain concentration[25,39,65]

$$\ln\left(\frac{I_0}{I}\right) = \frac{[Q]}{[M]} \tag{7}$$

where I_0 and I are the intensities of the first peak in emission spectra of pyrene, in the absence and the presence of the quencher, respectively; [Q] is the CPB concentration, and [M] is the concentration of the microdomains, in mM. The plots of $\ln(I_0/I)$ versus [Q] give straight lines (Figure 9) from the slope of which one can calculate [M] and then N_{agg} according to eq 8.

$$N_{agg} = \frac{c_H}{[M]} \tag{8}$$

where c_H is the concentration in hydrophobic groups, in mM.

In the case of polymers with pendant amphiphilic groups (polysoaps or brushed polymer), it may be that not all of the pendant hydrophobes are included in microdomains. Attempts to determine the fraction of hydrophobes involved in microdomains were done by different methods, the most recent by making use of NMR analysis.[25,36] It has been shown that the alkyl chain signals in ^{13}C NMR spectra are shifted downfield as a result of aggregation. Unfortunately, our attempts to use this method failed because the polymer concentrations to be tested (0.01−1 g/dL) were below the method's sensitivity. Therefore, we have calculated the N_{agg} under the assumption

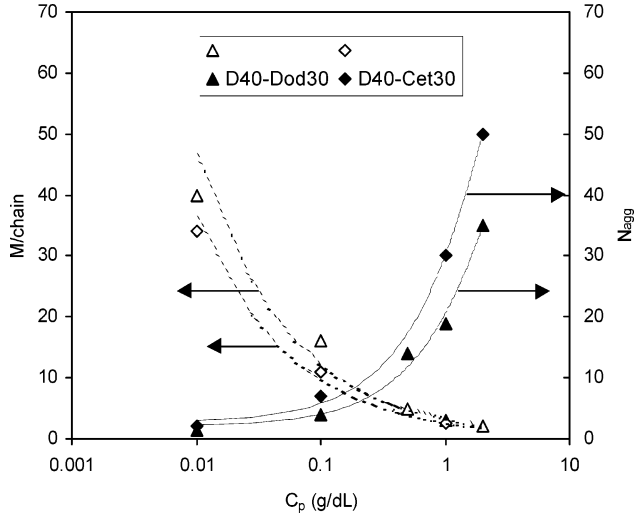

Figure 10. Variation of the aggregation number (N_{agg}) of the microdomains and the number of microdomains per chain (*M*/chain) as a function of cationic polymer concentration.

that all hydrophobes are involved in hydrophobic microdomains. This assumption might be true for polymers with higher degrees of substitution (15−30 mol %) where the density of the side alkyl chains is high enough. We have also calculated the average number of microdomains per polymer chain (*M*/chain), by relating the calculated [M] to the number of polymer chains corresponding to the polymer amount in the analyzed solution. This value is more accurate than N_{agg} because it does not take into account the real fraction of hydrophobes included in microdomains. Figure 10 shows the variation of N_{agg} and *M*/chain with the concentration of the most hydrophobic polymers studied, D40−Dod30 and D40−Cet30. At a concentration of 0.01 g/dL, corresponding to the offset of NPN and Py fluorescence response, the hydrophobes form a large number of very small aggregates (2−3 hydrophobes/aggregate). Increasing polymer concentration results in an increase in N_{agg} and a decrease in the number of aggregates per chain. Thus, at a concentration of 1−2 g/dL, the hydrophobes on a polymer chain are included in a few aggregates containing about 20−30 side chains. The values of N_{agg} and *M*/chain for several polymers at 1 g/dL are included in Table 2. From these values, we can conclude that at DS = 15−30 mol % all of the hydrophobes seem to be included in microdomains (*M*/chain > 1) and that these domains are of a rather small size, except for D40−Oct30 where much larger microdomains are formed. The N_{agg} (71) calculated for this polymer is very close to the number of hydrophobes per polymer chain (73), but this finding is not sufficient to prove a unimer formation. As we will also show, these microdomains can be formed with the participation of more than one chain (intermolecular association). When DS < 15 mol %, *M*/chain < 1, which is a possible indication of the existence of free hydrophobes, those not involved in microdomains. Thus, the corresponding calculated values for N_{agg} are overestimated.

The values obtained for N_{agg} of our polymers are lower than the values reported for other hydrophobically modified polyelectrolytes,[23,25,28] but a direct comparison is difficult due to differences in the chemical structure of polymers. A significant difference occurs in the concentration dependence of N_{agg} found in the present study, in comparison with the constant aggregation number reported for the polymers undergoing either intramolecular association,[23] or intermolecular association,[19] over a large concentration range. More experiments are necessary to clarify this finding.

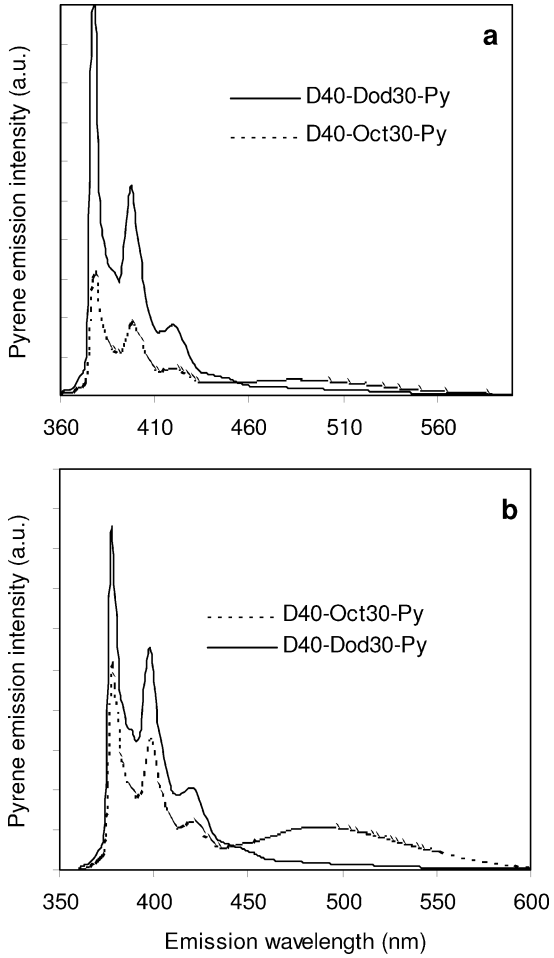

Figure 11. Emission fluorescence spectra of polymers labeled with pyrene (0.35 mole/chain) at polymer concentrations of 0.02 g/dL (a) and 2 g/dL (b).

Fluorescence of Pyrene-Labeled Polymers. In an attempt to discriminate between the intra- and intermolecular hydrophobic interactions, we prepared two cationic polymers of the type D40−Oct30−Py and D40−Dod30−Py containing an amount of pyrene label as low as 0.3−0.4 mol/chain. It was supposed that at this very low label content the intramolecular associations between two labels leading to excimer formation are completely avoided and only intermolecular ones could be noticed. The fluorescence emission spectra of the labeled polymers look different (Figure 11). In the case of the dodecyl-group-containing polymer, no excimer formation could be observed, even at polymer concentration as high as 2 g/dL; instead, for the octyl-group-containing polymer, the excimer peak occurs in a large concentration range of 0.02−2 g/dL. In the latter case, the ratio I_E/I_M varies from 0.1 (0.02 g/dL) to 0.25 (2 g/dL). No excimer formation was observed in the emission spectra of the pyrene bound to dextran in the absence of cationic amphiphilic pendant groups. Moreover, the intensity of the emission spectra for the bound pyrene differs very much for the two labeled polymers. Pyrene bound to the dodecyl-group-containing polymer shows a large increase in the intensity of the whole emission spectrum, whereas when bound to octyl-group-containing polymer, it has much lower emission intensity (Figure 11). All of these results suggest a different hydrophobe aggregation for the two polymers. The dodecyl-group-containing polymer forms only intramolecular aggregates, whereas pyrene is included as a monomer and senses a very hydrophobic environment, determining the large increase in emission intensity

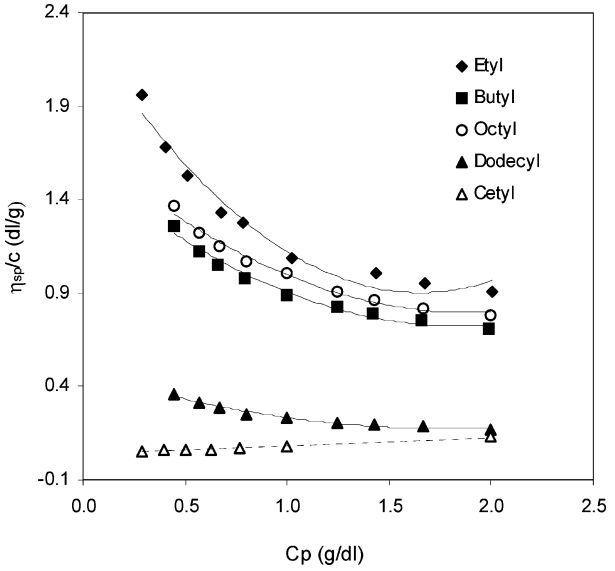

Figure 12. Huggins plots for the aqueous solutions of the polymer D40−R30, with different length of R. Temperature: 25 °C.

and the absence of the excimer peak. Some of the octyl groups in D40−Oct30−Py form intermolecular aggregates where two pyrene molecules bound to different chains can interact and form excimers, but these aggregates are loose and less hydrophobic, having, as a result, a low value for the pyrene emission intensity.

Viscosity Measurements. To support our conclusion about intra- and intermolecular aggregation of cationic amphiphilic polymers, we performed some viscometric measurements for the polymers having DS ≈ 30 mol %. The Huggins plots presented in Figure 12 show a different behavior of the polymers that have different alkyl chain substituents. Very hydrophilic polymers with ethyl and butyl groups have high viscosity and clear polyelectrolyte behavior (the increase of reduced viscosity with decreasing concentration). Very hydrophobic polymers with dodecyl and cetyl groups have much lower viscosity over all of the used concentration range, and D40−Cet30 showed no polyelectrolyte behavior, meaning that the electrostatic repulsion was completely suppressed by hydrophobic attractions between cetyl groups. The octyl-group-containing polymer has a different position because its viscosity is higher than that of the more hydrophilic polymer with butyl groups, over all of the concentration range. The association of the side chains of this polymer was already proven by fluorescence, and its higher viscosity suggests the presence of some intermolecular associations of the side octyl chain, which are not at all present in the case of the dodecyl and cetyl groups in the more hydrophobic polymers, in the range of concentrations used in this study. Kinematic viscosities of aqueous solutions containing 1 g/dL of such polymers are always very low, even when the degree of substitution is as low as 5 mol % (Table 2). However, the cationic polymers with 5−10 mol % content in dodecyl or cetyl substituents showed a deviation from linearity of the plots of reduced viscosity versus C_p at concentrations higher than 3−5 wt %, suggesting the occurrence of some intermolecular association (data not shown). This aspect will be studied in detail in a forthcoming paper.

Conclusions

Several fluorescence techniques and fluorescence probes have been used to characterize the hydrophobic microdomains formed by the side chains of polysaccharides carrying *N*-alkyl-*N*,*N*-dimethyl-*N*-(2-hydroxypropyl)ammonium chloride pendant groups in dilute aqueous solutions. All of the obtained results suggest a concentration dependence of the aggregation of the alkyl side groups. Below a certain concentration (cac_1), the polymers are in an extended form because of the electrostatic repulsion between the charged groups, and no significant association between the hydrophobic pendant groups is allowed. With increasing polyelectrolyte concentration above cac_1, the increase in ionic strength due to the increase in the concentration of charges determines a conformation change of the polymer chain to a less extended form, resulting in the association of hydrophobic side chains. This early state is sensed by fluorophores with different chemical structures and hydrophobicities and depends strongly on the polymer's chemical composition. By increasing polymer concentration, more small aggregates are formed along a polymer chain until almost all hydrophobes are included (cac_2). After that association processes do not stop, despite the offset of the fluorophore response (Py and NPN), but continues by an increase in the aggregate size. The increase in size takes place as a second-step aggregation, by association of very small aggregates into larger ones (the aggregation number increases, and the number of aggregates per chain decreases). No saturation of this process was found until a concentration of several orders of magnitudes beyond cac, but lower than overlapping concentration of native dextran. Apparently, these larger microdomains have a similar polarity and microviscosity to the small ones (DPH anisotropy is similar) but have much higher DPH solubilization ability than the initial aggregates.

The characteristics of the microdomains depend significantly on the length of the hydrophobic side chains and the content in this hydrophobe (degree of substitution). The microdomains are formed mainly intramolecularly, except for the polymers with octyl groups, which also form intermolecular aggregates, as proven by using labeled polymers and viscometric measurements.

The data obtained so far show some interesting properties of these new amphiphilic polyelectrolytes. An extension of the study to higher polymer concentrations and higher molecular weights of the polysaccharides could bring new insights into the aggregation process of this type of polymer.

Acknowledgment. We thank the FCT for financial support for the project POCTI/QUI/35413/2000 and for postdoctoral grant for M.N. (SFRH/BPD/5695/2001). M.N. is indebted to the Romanian Ministry of Education and Research for partial financial support (Ceres project C1/132/2001).

References and Notes

(1) *Hydrophilic Polymers: Performance with Environmental Acceptance*; Glass, J. E., Ed.; Advances in Chemistry Series 248; American Chemical Society: Washington, DC, 1996.

(2) *Water Soluble Polymers*; Shalaby, S. W., McCormick, C. L., Butler, G. B., Eds.; ACS Symposium Series 467; American Chemical Society: Washington, DC, 1991.

(3) Torchilin, V. P. *J. Controlled Release* **2001**, *73*, 137−172.

(4) Wang, I. D.; Gan, Q.; Shi, C. Y.; Zheng, X. L.; Yang, S. H.; Li, Z. M.; Dai, Y. Y. *Chem. Eng. J*. **2002**, *88*, 95−101.

(5) Kötz, J.; Kosmella, S.; Beitz, T. *Prog. Polym. Sci*. **2003**, *26*, 1199−1232.

(6) Strauss, U. P. In *Interaction of Surfactants with Polymer and Proteins*; Goddard, E. D., Anathapadmanabhan, K. P., Eds.; CRC Press: New York, 1993; pp 277−293.

(7) Tiera, M. J.; de Oliveira Tiera, V. Ap.; de Toledo, E. C.; de Sena, G. L. *Colloid Polym. Sci*. **2000**, *278*, 1052−1060.

(8) Mizusaki, M.; Morishima, Y.; Winnik, M. F. *Macromolecules* **1999**, *32*, 4317−4326.

(9) Morimoto, H.; Hashidzume, A.; Morishima, Y. *Polymer* **2003**, *44*, 943−952.

(10) Chang, Y.; McCormick, C. L. *Macromolecules* **1993**, *26*, 6121−6126.
(11) Cochin, D.; De Schreyver, F. C.; Laschevsky, A.; van Stam, J. *Langmuir* **2001**, *17*, 2579−2584.
(12) Laschewsky, A. *Curr. Opin. Colloid Interface Sci*. **2003**, *8*, 274−281.
(13) Kotzev, A.; Laschewsky, A.; Adriaensens, P.; Gelan, J. *Macromolecules* **2002**, *35*, 1091−1101.
(14) Morishima, Y.; Nomura, S.; Ikeda, T.; Seki, M.; Kamachi, M. *Macromolecules* **1995**, *28*, 2874−2881.
(15) Yusa, S.; Kamachu, M.; Morishima, Y. *Langmuir* **1998**, *14*, 6059−6067.
(16) Lee, K. Y.; Jo, W. H.; Kwon, I. C.; Kim, Y. H.; Jeong, S. Y. *Macromolecules* **1998**, *31*, 378−383.
(17) Nagayama, T.; Hashidzume, A.; Morishima, Y. *Langmuir* **2002**, *18*, 6775−6782.
(18) Smith, G. L.; McCormick, C. L. *Macromolecules* **2001**, *34*, 5579−5586.
(19) Noda, T.; Morishima, Y. *Macromolecules* **1999**, *32*, 4631−4640.
(20) Esquenet, C.; Buhler, E. *Macromolecules* **2001**, *34*, 5287−5294.
(21) Miyazawa, K.; Winnik, F. M. *Macromolecules* **2002**, *35*, 9536−9544.
(22) Damas C.; Adnibnejad, M.; Behjellun, A.; Brembilla A.; Carre, M. C.; Viriot, M. L.; Lochon, P. *Colloid Polym. Sci*. **1997**, *275*, 364−371.
(23) Binana-Limbelé, W.; Zana, R. *Macromolecules* **1990**, *23*, 2731−2739.
(24) Anthony, O.; Zana, R. *Macromolecules* **1994**, *27*, 3885−3891
(25) Petit-Agnely, F.; Iliopoulos, I.; Zana, R. *Langmuir* **2000**, *16*, 9921−9927.
(26) Bromberg, L. E.; Barr, D. P. *Macromolecules* **1999**, *32*, 3649−3657.
(27) Leddet, C.; Fischer, A.; Bembilla, A.; Lochon, P. *Polym. Bull*. **2001**, *46*, 75−82.
(28) Yusa, S.; Sakakibara, A.; Yamamoto, T.; Morishima, Y. *Macromolecules* **2002**, *35*, 10182−10188.
(29) McCormick, C. L.; Chang, Y. *Macromolecules* **1994**, *27*, 2151−2158.
(30) Rouzes, C.; Durand, A.; Leonard, M.; Dellacherie, E. *J. Colloid Interface Sci*. **2002**, *253*, 217−223.
(31) Raju, B. B.; Winnik, F. M.; Morishima, Y. *Langmuir* **2001**, *17*, 4416−4421.
(32) Mizusaki, M.; Morishima, Y.; Raju, B. B.; Winnik, F. M. *Eur. Phys. J. E* **2001**, *5*, 105−115.
(33) Bai, G.; Santos, L. M. N. B. F.; Nichifor, M.; Lopes, A.; Bastos, M. *J. Phys. Chem. B* **2004**, *108*, 405−413.
(34) Priev, A.; Zalipsky S.; Cohen, R.; Barenholz, Y. *Langmuir* **2002**, *18*, 612−617.
(35) Senan, C.; Meadows, J.; Shone, P. T.; Williams, P. A. *Langmuir* **1994**, *10*, 2471−2479.
(36) Petit-Agnely, F.; Iliopoulos, I. *J. Phys. Chem. B* **1999**, *103*, 4803−4808.
(37) Turner, M. S.; Joanny, J. F. *J. Phys. Chem*. **1993**, *97*, 4825−4831.
(38) Dobrynin, A. V.; Rubinstein, M. *Macromolecules* **2000**, *33*, 8097−8105.
(39) Winnik, F. M.; Regismond, S. S. T. *Colloids Surf., A* **1996**, *118*, 1−39
(40) Capek, I. *Adv. Colloid Interface Sci*. **2002**, *97*, 91−149.
(41) Prazeres, T. J. V.; Beingessner, R.; Duhamel, J. *Macromolecules* **2001**, *34*, 7876−7884.
(42) Azumi, T.; McGlynn, S. T. *J. Chem. Phys*. **1962**, *37*, 3413−3418.
(43) Sedgwick, E. G.; Bragg, P. D. *FEBS Lett.* **1988**, *229*, 127−130.
(44) Goni, F.; Alonso, A. *Biochim. Biophys. Acta* **2000**, *1508*, 51−68.
(45) Cajal, Y.; Busquets, M. A.; Carjaval, H.; Girona, V.; Alsina, M. A. *J. Mol. Catal. B: Enzym.* **2003**, *22*, 315−328.
(46) Brito, R. M. M.; Vaz, W. L. C. *Anal. Biochem*. **1986**, *152*, 250−255.
(47) Nichifor, M.; Lopes, A.; Carpov, A. Melo, E. *Macromolecules* **1999**, *32*, 7078−7085.
(48) Kalyanasundaram, K.; Thomas, J. K. *J. Am. Chem. Soc*. **1977**, *99*, 2039−2044.
(49) Wilhelm, M.; Zhao, Ch-L.; Wang, Y.; Xu, R.; Winnik, M.; Mura, J.-L.; Ries, G.; Croucher, M. D. *Macromolecules* **1991**, *24*, 1033−1040.
(50) Astafieva, I.; Zhong, X. F.; Eisenberg, A. *Macromolecules* **1993**, *26*, 7339−7352.
(51) Anghel, D. F.; Toca-Herrera, J. L.; Winnik, F. M.; Retting, W.; v. Klitzing, R. *Langmuir* **2002**, *18*, 5600−5606.
(52) Kanagalingam, S.; Ngan, C. F.; Duhamel, J. *Macromolecules* **2002**, *35*, 8560−8570.
(53) Yamazaki, A.; Song, J. M.; Winnik, F. M.; Brash, J. L. *Macromolecules* **1998**, *31*, 109−115.
(54) Pruitt, J. D.; Husseini G.; Rapoport, N.; Pitt, W. G. *Macromolecules* **2000**, *33*, 9306−9309.
(55) Selb, J.; Biggs, S.; Renoux, D.; Candau, F. In *Hydrophilic Polymers: Performance with Environmental Acceptance*; Glass, J. E., Ed.; Advances in Chemistry Series 248; American Chemical Society: Washington, DC, 1996; pp 251−278.
(56) Oosawa, F. *Polyelectrolytes*; Marcel Dekker: New York, 1971.
(57) Beoudoin, E.; Hiorns, R. C.; Borisov, O.; François, J. *Langmuir* **2003**, *19*, 2058−2066.
(58) Lopes, A.; Maçanita, A.; Pina, F. S.; Melo, E.; Wamhoff, H. *Environ. Sci. Technol*. **1992**, *26*, 2448−2453.
(59) Kim, C.; Lee, S. C.; Kang, S. W.; Kwon, I. C.; Kim, Y. H.; Jeong, S. Y. *Langmuir* **2000**, *16*, 4792−4797.
(60) Leckband, D. E.; Borisov, O. V.; Halperin, A. *Macromolecules* **1998**, *31*, 2368−2374.
(61) Hansson, P.; Jönsson, B.; Ström, C.; Söderman, O. *J. Phys. Chem. B* **2000**, *104*, 3496−3506.
(62) Mukerjee, P.; Mysels, K. J. *Critical Micelle Concentrations of Aqueous Surfactant Systems*; U.S. Department of Commerce, U.S. Government Printing Office: Washington, DC, 1971.
(63) Bakeev, K. N.; Ponomarenko, E. A.; Shishkanova, T. V.; Tirrell, D. A.; Zezin, A. B.; Kabanov, V. A. *Macromolecules* **1995**, *28*, 2886−2892.
(64) Colby, R. H.; Plucktaveesak, N.; Bromberg, L. *Langmuir* **2001**, *17*, 2937−2941.
(65) Moroi, Y. *Micelles: Theoretical and Applied Aspects*; Plenum Press: New York, 1992.